ELSEVIER

Polymer 43 (2002) 461–466

polymer

www.elsevier.com/locate/polymer

Three-dimensional simulations of diblock copolymer/particle composites ☆

Valeriy V. Ginzburg[1], Feng Qiu, Anna C. Balazs*

Department of Chemical and Petroleum Engineering, University of Pittsburgh, Pittsburgh PA 15261, USA

Abstract

We develop a coarse-grained model to investigate the influence of nanoscale particles on the phase separation and the morphology of symmetric AB diblock copolymer melts. The microphase separation is modeled by the cell dynamical systems (CDS) equations, while the particle dynamics is described by a Langevin equation. We assume that the particles have a selective affinity to the A block and thus, can self-assemble and form clusters within A-domains. By varying the particle volume fraction, ϕ_p, we study the coupling between the microphase separation of the diblocks and the cluster formation for the particles. We also estimate the percolation threshold, ϕ^*, for the particles and find that the presence of diblocks decreases ϕ^* by a factor slightly greater than two relative to the case of particles in a homopolymer ($\phi^* \approx 9\%$ in a diblock vs. 22% in a homopolymer). This result can be useful in designing new composites with increased electrical conductivity and/or mechanical strength.

Keywords: Copolymer; Macromolecules; Computer simulation

1. Introduction

The majority of high-performance polymers involve a blend of macromolecules and solid 'filler' particles, which serve to improve the properties of the polymeric matrix. Recently, there has been significant interest in the development of composites where the polymeric matrix is composed of block copolymers. For example, a composite consisting of a diblock polyelectrolyte and carbon black nanoparticles was shown to exhibit improved electric conductivity and mechanical stability, making it an optimal material for solid-state rechargeable batteries [1]. As another example, a mixture of diblock copolymers with clay nanoparticles yielded new polymer/clay nanocomposites with increased mechanical strength and toughness; in particular, adding only 5 wt% of clay to the copolymer increased the tensile modulus 1.4 times [2]. Block copolymers were also used as 'templates' to control the deposition of metal particles onto thin films [3–5]. Such diblock/particle mixtures are now being synthesized for the use in photonic band gap devices [6].

While there have been a number of experimental studies on fabricating diblock/particle composites [3–9], there have been few theoretical investigations into the factors that control the thermodynamic and kinetic behavior of these systems. Recently, however, several numerical methods were used to allow researchers to study the morphology and properties of such systems. Among these methods are the lattice Monte-Carlo technique [10], dynamical density functional theory [11], and a hybrid cell dynamical system method [12,13]. These approaches made it possible to study the interplay between the diblock microphase separation and the self-assembly and clustering of the nanoparticles.

In our recent studies [10,13], we concentrated on the behavior of AB-diblock copolymers mixed with spherical nanoparticles (P). The particles had a strong preferential affinity toward the A-block. This preferential interaction can be achieved, for example, by grafting short A-chains on the surface of each particle. We calculated the phase diagram for this system in the strong segregation limit [10] and found that when the particle size was slightly smaller than the radius of gyration of the A-block, the particles could self-assemble into 'nanowires' or 'nanosheets' within the A-phase. These calculations were qualitatively confirmed by Monte-Carlo simulations [10] and by two-dimensional hybrid dynamic simulations [13].

In this paper, we expand the hybrid method of Ref. [13] to three dimensions. The paper is structured as follows. In Section 2, we derive our equations of motion, describe the numerical method and the systems to be studied. In Section 3, we discuss the simulation results. Finally, Section 4 contains conclusions and directions for future work.

☆ This paper was originally submitted to *Computational and Theoretical Polymer Science* and received on 11 November 2000; received in revised form on 28 February 2001; accepted on 28 February 2001. Following the incorporation of *Computational and Theoretical Polymer Science* into *Polymer*, this paper was consequently accepted for publication in *Polymer*.

* Corresponding author.

E-mail address: balazs@vms.cis.pitt.edu (A.C. Balazs).

[1] Present address: The Dow Chemical Company, Building 1702, Midland, MI 48674, USA.

0032-3861/02/$ - see front matter
PII: S0032-3861(01)00428-1

2. Model

We represent the polymer melt by a three-dimensional square lattice, which is $64 \times 64 \times 64$ sites in size and has periodic boundary conditions in all three directions. On each lattice site, we define the scalar order parameter $\Psi = \rho_A - \rho_B$, where ρ_A and ρ_B are the respective local densities of the A and B components. Note that $\Psi = 1$ (-1) corresponds to the equilibrium order parameter for the A-rich (B-rich) phase. Into this system, we introduce spherical particles of radius $R_0 = 1$. The particles have an affinity for the A block. This affinity is introduced via the boundary conditions on the surface of each particle and a polymer–particle coupling term in the free energy (as described below). Thus, the particles can influence the morphology and size of the polymer domains that are formed during the microphase separation, and the polymers can affect the spatial distribution of the particles. Below, we describe the equations of motion for both the polymeric and the particulate components.

The dynamics of microphase separation in a melt of diblocks can be described through the following equation [14–16]:

$$\frac{\partial \Psi}{\partial t} = M\nabla^2 \frac{\delta \mathscr{F}}{\delta \Psi} - \Gamma(\Psi - F) + \xi. \tag{1}$$

The constant M is the mobility for the order parameter field. The variable $F = 2f - 1$ describes the asymmetry of the diblock; for a symmetric diblock, $f = 0.5$, and $F = 0$. The ξ term is the noise field (which we set to zero in this study), and the parameter Γ determines the thickness of the lamellar domains and is proportional to $\mathscr{N}^{-2}$, where $\mathscr{N}$ is the length of the block copolymer [14,15].

The free energy $\mathscr{F}$ is given by:

$$\mathscr{F} = \mathscr{F}_l + \mathscr{F}_{\mathrm{cpl}}, \tag{2}$$

Here, the local free energy term $\mathscr{F}_l$ is given by:

$$\mathscr{F}_l = \int \mathrm{d}r \left[f_l(\Psi(r)) + \frac{D}{2}(\nabla \Psi)^2 \right], \tag{3}$$

where the double well potential f_l is selected to be,

$$f_l = -A \log(\cosh(\Psi)) + \frac{1}{2}\Psi^2. \tag{4}$$

The coupling term $\mathscr{F}_{\mathrm{cpl}}$ describes the interactions between the particles and the polymer. To model this term, we select the following expression:

$$\mathscr{F}_{\mathrm{cpl}} = C \int \mathrm{d}r \sum_i V(r - R_i)(\Psi(r) - \Psi_s)^2, \tag{5}$$

where $\Psi_s = 1$ is the value of the order parameter at the particle surface. The potential $V(r)$ is assumed to be exponential (although any other rapidly decaying function could also be used)

$$V(r) = \exp\left(-\frac{r}{r_0}\right). \tag{6}$$

We set the 'coupling range' $r_0 = 3$, so the interaction is short-ranged. (It only affects the nearest and next-nearest neighbor sites for a given particle.)

The motion of the particles is described by the Langevin equation:

$$\dot{R}_i = M_p\left(f_i - \frac{\partial \mathscr{F}}{\partial R_i}\right) + \eta_i, \tag{7}$$

where M_p is the particle mobility, f_i is the force acting on the ith particle due to all the other particles, and η represents a Gaussian white noise with $\langle \eta_{i\alpha}(r,t)\eta_{j\beta}(r',t')\rangle = G_2\delta(r - r')\delta(t - t')\delta_{ij}\delta_{\alpha\beta}$. In this study, we neglect interactions between particles (i.e. $f_i = 0$) and consider only the particles' diffusive motion and their interaction with the polymer.

A cell dynamical systems (CDS) method [15,17,18] is used to update the value of Ψ for the phase-separating AB mixture. By employing CDS modeling (rather than a conventional discretization of Eq. (1)), we can significantly increase the computational speed of the simulation [19].

To simulate the particle dynamics, we discretize Eq. (7) and only allow the particles to move between different lattice sites. A 'Kawasaki exchange' mechanism is used for each particle move. First, the order parameter values from all the cells to be occupied by a particle in its 'new' position are moved to the 'old' position of the particle. Next, the boundary and excluded volume conditions are imposed for the order parameter at the new particle position. This mechanism ensures the conservation of the order parameter. Such dynamics may break down for high particle mobilities, so we only consider the case where the diffusion constant is relatively low (almost all particle 'jumps' are to neighboring sites). The discretized equations of motion have the following form:

$$\Psi(r, t+1) = F[\Psi(r,t)] - \langle\langle F[\Psi(r,t)] - \Psi(r,t)) \rangle\rangle, \tag{8}$$

$$f(\Psi) = A \tanh(\Psi),$$

$$F[\Psi(r,t)] = f(\Psi(r,t)) + \frac{\delta \mathscr{F}_{\mathrm{cpl}}}{\delta \Psi} + D(\langle\langle \Psi(r,t) \rangle\rangle - \Psi(r,t)),$$

$$R_i(t+1) = R_i(t) + M_p\left(f_i - \frac{\partial \mathscr{F}}{\partial R_i}\right) + \eta_i(t),$$

where $\langle\langle * \rangle\rangle$ is the isotropic spatial average over the nearest-neighbor and the next-nearest neighbor sites, and $[\langle\langle * \rangle\rangle - *]$ can be thought of as a discrete generalization of the Laplacian.

At the surface of each particle, the lattice boundary conditions (specified order-parameter value and zero order-parameter flux) are imposed as: $\Psi(r,t) = \Psi_s$, and $\partial_n F(r,t) = 0$, if $R_0 < |r - R_i(t)| \le R_0 + a$, where a is the lattice spacing

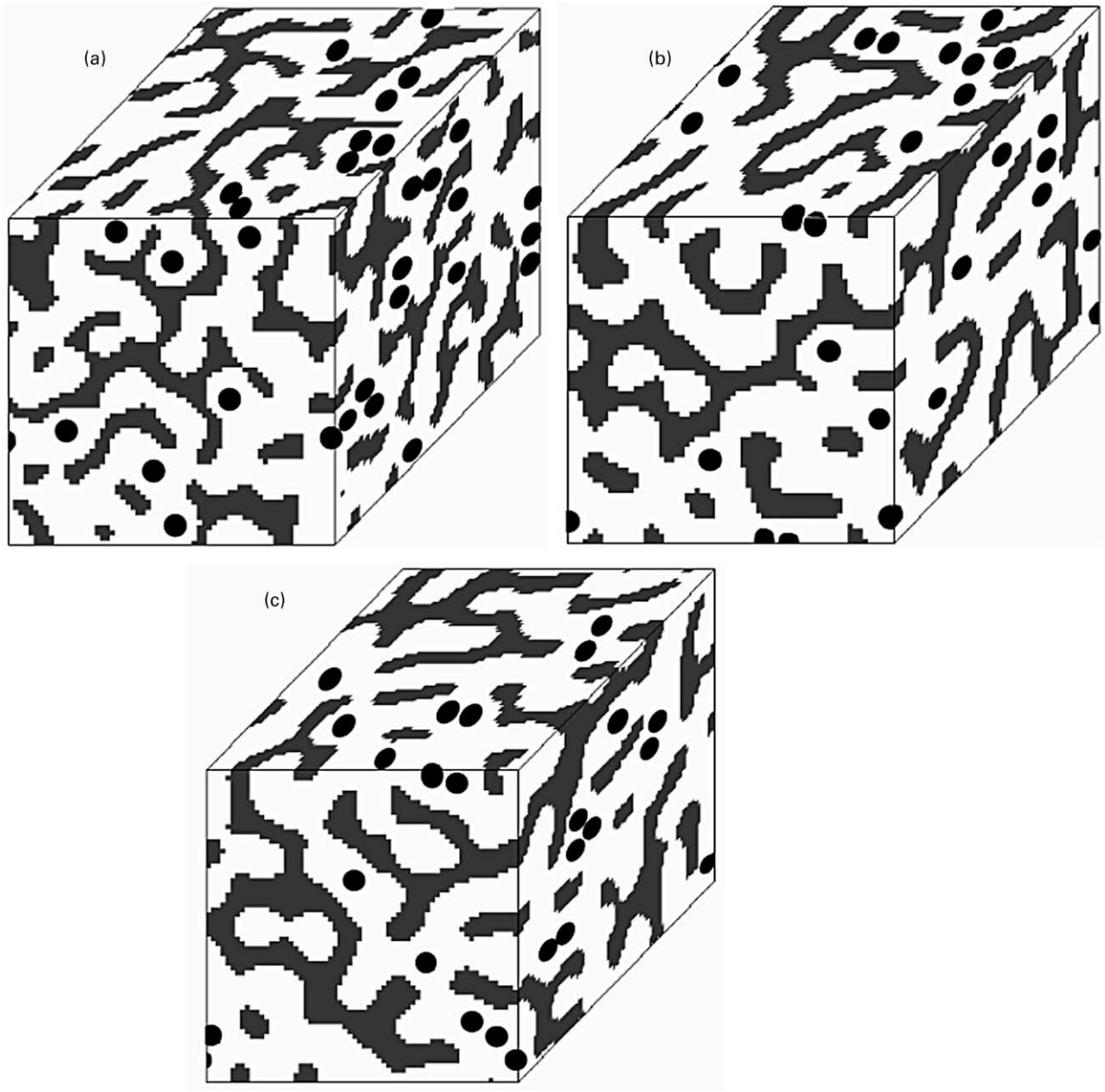

Fig. 1. Morphologies of the diblock copolymer/particle mixtures at early ($t = 1000$ timesteps, a), intermediate ($t = 10\,000$ timesteps, b), and late ($t = 100\,000$ timesteps, c) stages of microphase separation for the system with $N = 200$ particles ($\phi_p = 0.062$). The white areas correspond to the A-rich regions, the dark areas correspond to the B-rich regions, and the black ellipses represent particles.

and ∂_n denotes the 'lattice' normal derivative. Here, we set $\Psi_s = 1$ so that the particles are 'coated' by fluid A.[2] The $\partial_n F = 0$ condition ensures zero flux of Ψ into the particles since F plays the role of a chemical potential.

We use the following values of parameters: $A = 1.3$, $D = 0.5$, $G_1 = 0$, $G_2 = 0.5$, $\Gamma = 0.004$,[3] $f = 0.5$, and vary only the particle number, N. These parameters correspond to an intermediate-to-strong segregation regime for the diblocks. In our previous two-dimensional studies, we investigated the role of coupling interactions by varying the coupling constant C. It was found [12,13] that for the small values of C ('weak coupling case'), the particle motion was predominantly diffusive, and the particles disturbed the lamellar ordering of the diblocks. For large values of C ('strong coupling case'), the particles self-assembled into clusters inside the A-block. In the present study, we concentrate on the strong coupling case, setting $C = 0.05$. The case $C = 0$ is used as a benchmark to determine the particle behavior in the absence of the diblocks'

[2] The effective volume of each particle, together with its boundary layer, equals 81 lattice sites.

[3] This value of Γ corresponds to effective chain length $\mathcal{N} \approx 100$, according to the following equation: $\Gamma = 12/(f(1-f)\mathcal{N}^2)$ [14].

influence (since the particle behavior is purely diffusive, the particle cluster size distribution is independent of the surrounding polymeric fluid).

3. Results and discussion

We consider the case of symmetric diblocks ($f = 0.5$) and vary the number of particles $N = 0$, 100, 200, 300, and 400 (which corresponds to changing the particle volume fraction, ϕ_p, from 0 to 0.124). Starting from the initial random configuration (with diblocks in the disordered state), we let the system evolve and observe the process of microphase separation. The evolution of the system with $N = 200$ particles ($\phi_p = 0.062$) is shown in Fig. 1. The particles diffuse into the A-rich domains and increase the size of these regions compared to the case of pure diblock. The system shows some elements of lamellar ordering on a short scale; however, due to the small box size and periodic boundary conditions, the lamellae are interconnected, and the overall morphology is closer to a bicontinuous structure.

To characterize the dynamics of the microphase separation, we plot the characteristic lamellar thickness R, calculated using the Ohta–Jasnow–Kawasaki [20] equation:

$$R = \frac{L^d}{n_x + n_y + n_z}, \tag{9}$$

where $d = 3$ is the system dimensionality, L is the system size, and n_x, n_y, n_z are the numbers of 'broken bonds' counted in X, Y, or Z direction, respectively. The dependence of R on t is plotted in Fig. 2. We can see that the particles swell the A-lamellae, so the characteristic size increases with increasing N. This result is in agreement with our earlier simulations for the two-dimensional case in the strong-coupling limit. Note that the characteristic size depends linearly on the number of particles, which is consistent with previous simulations and experimental data (see Ref. [13] for more details).

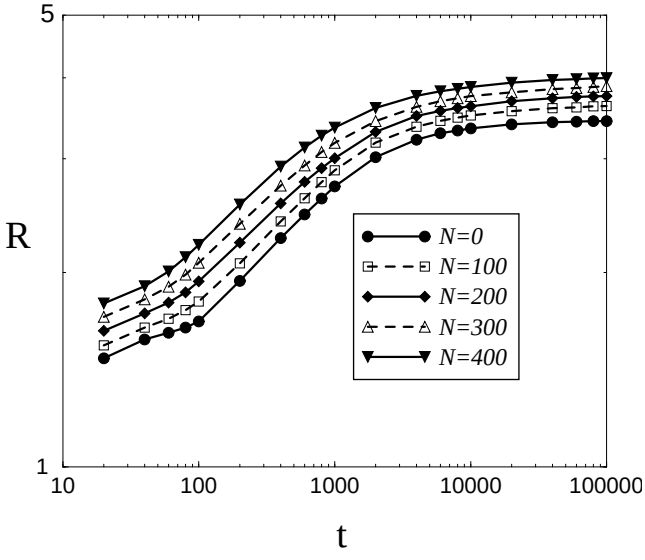

Fig. 2. Characteristic domain size as a function of time.

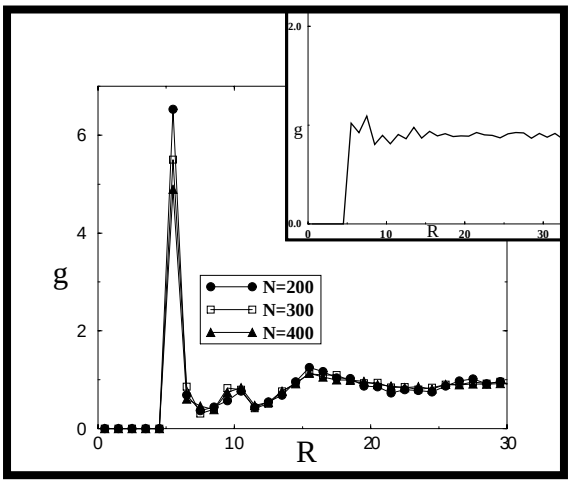

Fig. 3. Circularly-averaged particle pair correlation function $g(R)$ for the case $C = 0$, $N = 400$ (inset) and for the case $C = 0.05$, $N = 200$, 300, and 400.

We now turn our attention to the behavior of the particles. In Fig. 3, we show the pair correlation function at time $t = 100\,000$ timesteps for the systems with $N = 200$, 300, and 400 particles. It can clearly be seen that the correlation functions for these three cases are almost identical. In addition to the strong peak at separation $R = 6$, there are two smaller peaks at $R = 11$ and $R = 16$, dictated by the ordering of the diblock copolymer. These peaks are due to the correlation between the particles in the adjacent A-lamellae. When the interaction between the particles and the diblock

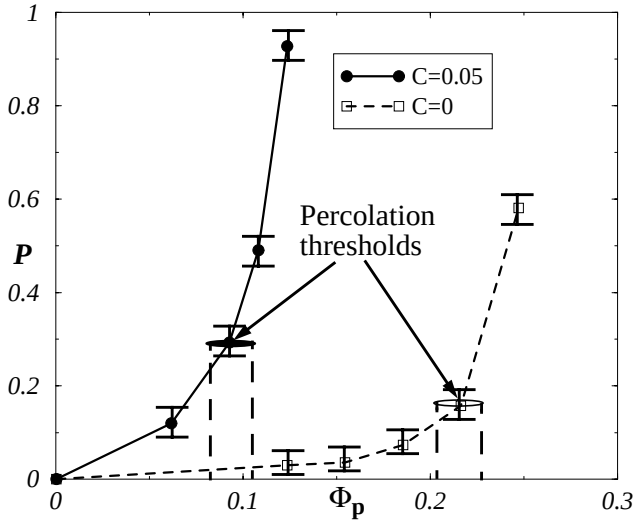

Fig. 4. Fraction of particles that belong to the largest cluster, $\mathscr{P}$, as a function of the particle volume fraction, ϕ_p. The solid curve corresponds to the case $C = 0.05$ ('strong coupling'), the dashed curve corresponds to the case $C = 0$ ('no coupling'). The arrows indicate the estimated percolation thresholds for both cases. The percolation threshold for the $C = 0$ case is the same as in the absence of the diblocks.

is turned off, both secondary peaks disappear, as one would expect (see inset, calculated for $N = 400$, $C = 0$).

Although the pair correlation function for the particles is relatively insensitive to their volume fraction, the global arrangement of the particles depends on ϕ_p is a critical way. We can characterize this arrangement qualitatively by measuring $\mathscr{P}$, the fraction of particles that belong to the largest cluster. When $\mathscr{P}$ is close to 1, almost all the particles belong to one cluster; when $\mathscr{P}$ is close to 0, the particles form many small clusters. It can be seen (Fig. 4) that the strong interaction of the particles with the diblocks significantly increases $\mathscr{P}$ for a given particle volume fraction ϕ_p.

We can now estimate the percolation threshold, ϕ_p^*, for our system. To do that, we examine the largest cluster for each volume fraction and check whether it extends between any two opposing edges of the simulation box. The estimated percolation thresholds are shown in Fig. 4 with two arrows (for the 'no-coupling case' $C = 0$ and the 'strong-coupling case' $C = 0.05$). The $C = 0$ case is equivalent to the absence of any polymer, since the motion of the particles is governed purely by the random Brownian forces. In the $C = 0.05$ case, on the other hand, particles are strongly confined within the A-rich regions by the 'coupling' forces. As a result, they have much smaller translational freedom, and interact with each other more often. All this leads to a significant decrease in the percolation threshold. While for the $C = 0$ case we find $\phi_p^* \approx 0.22 \pm 0.02$, for the $C = 0.05$ case, the result is $\phi_p^* \approx 0.09 \pm 0.02$. Thus, by using symmetric diblock copolymers instead of homopolymers, one can reduce the percolation threshold for the fillers by a factor of 2.

This result can be easily understood by using the 'double percolation' model, first developed to describe the behavior of carbon black particles in binary polymer blends [21–24]. According to this model, the filler particles can percolate and form infinite conducting clusters if two conditions are satisfied: (i) the $(A + P)$ phase is continuous, and (ii) the particles percolate within the $(A + P)$ phase. These conditions can be written as:

$$\phi_p + f(1 - \phi_p) \geq 0.5, \tag{10}$$

$$\frac{\phi_p}{\phi_p + f(1 - \phi_p)} \geq p_c, \tag{11}$$

where p_c is the bulk percolation threshold for spherical particles. We estimated $p_c \approx 0.23 \pm 0.02$.[4] By looking at Eqs. (10)–(11), one can clearly see that if the effective $(A + P)$ volume fraction is close to 0.5, the effective percolation threshold decreases roughly two times compared to the case of fillers in a homopolymer matrix. This result is consistent with our simulations (Fig. 4), in which the effective percolation threshold for the particles in the symmetric AB-diblock was found to be 0.09 ± 0.01.

We performed several simulations with various diblock compositions ($f = 0.4, 0.6$) and found that the percolation threshold is relatively insensitive to the exact value of f as long as it does not deviate too far from 0.5, and the overall volume fraction of the $(A + P)$-phase is close to 0.5. Thus, the effect of lowering the percolation threshold by using diblock copolymers is expected to be relatively robust (as long as the nanoparticles are smaller than the equilibrium lamellar thickness for the A-block).

Finally, it is worth mentioning that the percolation threshold can be decreased even further by changing the shape of the fillers from spheres to rods. Our recent simulations of rods in phase-separating binary *blends* [25] showed that the percolation threshold is inversely proportional to the rod length (or aspect ratio) and that the phase separation between the two components, A and B, decreased the value of the percolation threshold by a factor of 2 compared to that of rods in a homopolymer matrix.

4. Conclusions

We performed three-dimensional dynamical simulations of diblock copolymer/particle mixtures, using a hybrid mesoscopic model that combines a CDS approach for the diblocks with Langevin dynamics for the particles. The particles had a strong preferential affinity toward one of the blocks (A), and the diblocks were in the limit of intermediate-to-strong segregation. The initial configuration was a mixed (disordered) state, and the system evolved toward microphase separated morphologies, with particles self-assembling within the A-rich regions. To characterize the dynamics of the process, we measured the effective domain size as a function of time and the particle volume fraction. As in our earlier, two-dimensional simulations [13], an increase in the particle volume fraction led to the swelling of the domains and the effective increase in the domain size. This result, as we discussed earlier [13], is applicable for the cases when the affinity of the particles toward one of the phases is sufficiently strong compared to kT.

The simulation method also allowed us to describe the self-assembly of particles into clusters. This process is especially important for the physical properties of the resulting composite, such as electrical conductivity or mechanical strength. We measured the size of the largest cluster for several particle volume fractions and estimated the approximate percolation threshold. Based on the simulations, we concluded that the use of diblocks instead of homopolymers could decrease the effective percolation threshold by roughly a factor of two. This result was in a qualitative agreement with the 'double percolation' model proposed earlier for the behavior of particles in binary blends. Furthermore, we suggested that percolation threshold

[4] The site percolation threshold for the simple cubic lattice is equal to 0.31 [24], which is somewhat higher than our estimate of 0.22 ± 0.02; the discrepancy may be due to the fact that our particles occupy more than one lattice site.

could be decreased even further by using anisotropic (rodlike) nanoparticles. The above results can be useful in developing new conducting polymer/inorganic nanocomposites.

Acknowledgements

This work was supported by the NSF, through Grant DMR0709101, DOE, through Grant DE-FG02-90ER-45438, and ONR, through Grant N00014-91-J-1363.

References

[1] Soo PP, Huang BY, Jang YI, Chiang YM, Sadoway DR, Mayes AM. J Electrochem Soc 1999;146:32.
[2] Hasegawa N, Okamoto H, Kawasumi M, Usuki A. J Appl Polym Sci 1999;74:3359.
[3] Morkved TL, Wiltzius P, Jaeger HM, Grier DG, Witten TA. Appl Phys Lett 1994;64:422.
[4] Lin BH, Morkved TL, Meron M, Huang ZQ, Viccaro PJ, Jaeger HM, Williams SM, Schlossman ML. J Appl Phys 1999;85:3180.
[5] Zehner RW, Lopes WA, Morkved TL, Jaeger H, Sita LR. Langmuir 1998;14:241.
[6] Fink Y, Urbas AM, Bawendi MG, Joannopoulos JD, Thomas EL. J Lightwave Technol 1999;17:1963.
[7] Cole DH, Shull KR, Baldo P, Rehn L. Macromolecules 1999;32:771.
[8] Hamdoun B, Ausserre D, Cabuil V, Joly S. J Phys II France 1996;6:493 see also pages 503, 1207.
[9] Lauter-Pasiuk V, Lauter HJ, Ausserre D, Gallot Y, Cabuil V, Hamdoun B, Kornilov EI. Physica B 1998;1092:241–3.
[10] Huh J, Ginzburg VV, Balazs AC. Macromolecules 2000;33:8085.
[11] Sevink GJA, Zvelindovsky AV, van Vlimmeren BAC, Maurits NM, Fraaije JGEM. J Chem Phys 1999;110:2250.
[12] Balazs AC, Ginzburg VV, Qiu F, Peng G, Jasnow D. J Phys Chem B 2000;104:3411.
[13] Ginzburg VV, Gibbons C, Qiu F, Peng G, Balazs AC. Macromolecules 2000;33:6140.
[14] Ohta T, Kawasaki K. Macromolecules 1986;19:2621.
[15] Oono Y, Bahiana M. Phys Rev Lett 1988;61:1109.
[16] Glotzer SC, DiMarzio EA, Muthukumar M. Phys Rev Lett 1995;74:2034.
[17] Oono Y, Puri S. Phys Rev A 1988;38:434 see also pages 1542.
[18] Hamley IW. Macromol Theory Simul 2000;9:363 and references therein.
[19] Ginzburg VV, Paniconi M, Qiu F, Peng G, Jasnow D, Balazs AC. Phys Rev Lett 1999;82:4026.
[20] Ohta T, Jasnow D, Kawasaki K. Phys Rev Lett 1982;49:1223.
[21] Sumita M, Sakata K, Asai S, Miyasaka K, Nakagawa H. Polym Bull 1991;25:265.
[22] Sumita M, Sakata K, Hayakawa Y, Asai S, Miyasaka K, Tanemura M. Colloid Polym Sci 1992;270:134.
[23] Sumita M, Sakata K, Asai S, Miyasaka K, Nakagawa H. Polym Bull 1991;25:265.
[24] Lux F. J Mater Sci 1993;28:285 and references therein.
[25] Peng G, Qiu F, Ginzburg VV, Jasnow D, Balazs AC. Science 2000;288:1802.